UNIVERSITY *of York*

This is a repository copy of *Order Parameters, Orientational Distribution Functions and Heliconical Tilt Angles of Oligomeric Liquid Crystals*.

White Rose
university consortium
Universities of Leeds, Sheffield & York

eprints@whiterose.ac.uk
https://eprints.whiterose.ac.uk/

PCCP

Accepted Manuscript

Volume 18 | Number 1 | 7 January 2016 | Pages 1–636

PCCP

Physical Chemistry Chemical Physics
www.rsc.org/pccp

ISSN 1463-9076

PERSPECTIVE
Darya Radziuk and Helmuth Möhwald
Ultrasonically treated liquid interfaces for progress in cleaning and separation processes

175 YEARS

ROYAL SOCIETY OF CHEMISTRY

rsc.li/pccp

ARTICLE

Order Parameters, Orientational Distribution Functions and Heliconical Tilt Angles of Oligomeric Liquid Crystals

Richard J. Mandle [a]* and John W. Goodby [a]

Twist-bend (TB) phases possess a local helical structure with a pitch length of a few nanometers. The TB phase was first observed in low molecular weight dimers, and as such these have been the focus of efforts to understand the properties and structure of these new phases of matter. Recently several oligomeric and polymeric materials have been reported, but there is little information on the properties and structure of the TB phase in these materials. Herein we compare the order parameters, orientational distribution functions (ODF) and heliconical tilt angles of the TB phase exhibited by a liquid-crystalline dimer (CB7CB) to a tetramer (O4$_7$) and hexamer (O6$_7$) by SAXS/WAXS. Following the N-TB phase transition we find that all order parameters decrease, and while $\langle P_2 \rangle$ remains positive $\langle P_4 \rangle$ becomes negative. For all three materials the order parameter $\langle P_6 \rangle$ is near zero in both phases. The ODF is sugarloaf-like in the nematic phase and volcano-like in the TB phase, allowing us to estimate the heliconical tilt angle of each material and its thermal evolution. Surprisingly, the heliconical tilt angle appears to be largely independent of the material studied despite the differing number of mesogenic units.

Introduction

The nematic liquid crystal phase possesses only an average orientational organisation of its constituent molecules. A phase of matter analogous to the nematic phase but with an additional twist-bend deformation has recently been discovered. 1, 2 The twist-bend nematic (TB, Fig 1) phase has a helical local structure with a pitch of a few nanometers, 3-6 spontaneously separating into domains of opposite handedness. 7 The structure of this phase is shown in Fig 1a. A smectic analogue of the TB phase has also been recently reported. 8 The TB phase was first observed in liquid-crystalline dimers, in which two mesogenic units are appended to a flexible methylene spacer unit of odd parity. 9 There are also examples of oligomeric (i.e. n-mers containing n mesogenic units), 10-14 polymeric 15, 16 and bent-core materials exhibiting this phase. 17, 18 The majority of studies on the local structure and bulk properties (such as pitch length, heliconical angle, order parameters) of the TB phase are on simple dimers, notably the CBnCB materials. Although some experimental work suggests that the overall molecular bend and flexibility underpins the incidence of the TB phase in dimers, 19 it is presently unclear how, or even if, such bend affects the local structure and bulk properties. In terms of oligomeric liquid crystals there is little to no data on how (or if)

the properties of these materials differ from low molecular weight dimers.
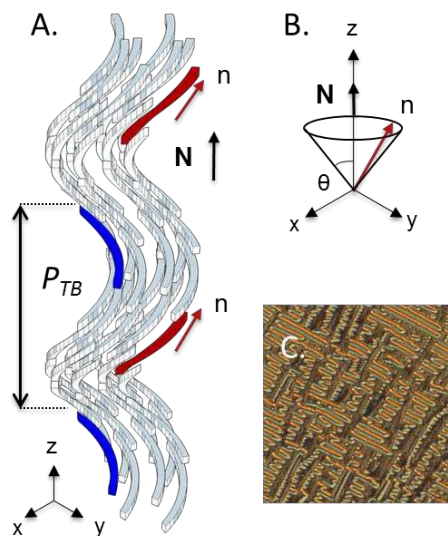
Fig 1: (A) Depiction of the structure of the twist-bend phase made up of curved rods with a ~ 100 ° bend. The pitch length (PTB) is indicated and is typically of the order of 10 nm. As shown in (B) the optic axis (N) of the TB phase is parallel to the helix axis (z), whereas the director (n, red arrow) is tilted away from z by the heliconical tilt angle (θ). (C) Photomicrograph (x100, crossed polarisers) of the tetramer **O4$_7$** in the TB phase at 100 °C.

Department of Chemistry, University of York, Heslington, York, YO10 5DD, UK
* Richard.mandle@york.ac.uk

Experimental

CB7CB was available in house and both the oligomeric materials **O4₇**, **O6₇** were synthesised as described previously; 20 their molecular structures and transition temperatures are given in Fig 2.

CB7CB Cr 100.4 TB 106.5 N 118.9 Iso

O4₇ (n = 2) Cr 143.9 TB 172.9 N 194.2 Iso
O6₇ (n = 4) Cr 174.4 TB 158.9 N 188.1 Iso

Fig 2: The molecular structures and transition temperatures (°C) of CB7CB, **O4₇** and **O6₇**.

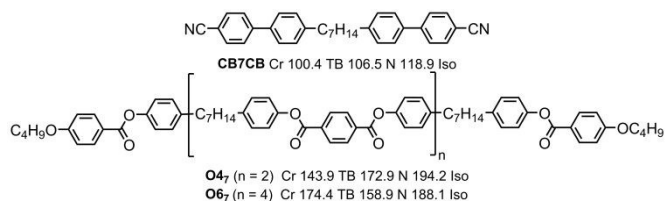We revisited these three materials with a view to using SAXS to extract additional information about the TB phase for these materials. These materials were selected as they each have the same spacer length (i.e. heptamethylene, -(CH₂)₇-) and this should minimise the effect of differing bend-angles and conformer populations when interpreting data. Order parameters ($\langle P_2 \rangle$, $\langle P_4 \rangle$ and $\langle P_6 \rangle$) were determined by small angle X-ray scattering (SAXS), using the method described in refs [21, 22]. This method requires an aligned sample and gives the orientational order parameters of the whole molecule.

The SAXS instrument employed was a Bruker D8 using CuK$_\alpha$ radiation. Each material was filled into a capillary tube (I.D. ~ 0.9 mm) which was placed into a bored graphite rod furnace providing temperature control of at least ± 0.1 °C. Alignment of the sample was obtained by an external magnetic field (~0.6 T) perpendicular to the incident X-ray beam. Each sample was cooled from the isotropic liquid until crystallisation, with frames recorded at regular temperature intervals. Separately, the 2D SAXS pattern obtained from an empty glass capillary in the sample holder was used as a background, and this was subtracted from the raw 2D SAXS data. Following background subtraction we performed azimuthal integration; fitting of this data according to the Kratky method yields the order parameters $\langle P_2 \rangle$ and $\langle P_4 \rangle$, as described elsewhere, *via* Equations 1-5. [21, 22]

$$I(X) = \sum_0^\infty f_{2n} \frac{2^n n!}{(2n+1)!!} cos^{2n} X \qquad (1)$$

$$\langle cos^2 \beta \rangle = \sum_{n=0}^\infty \frac{f_{2n}}{2n+3} \Big/ \sum_{n=0}^\infty \frac{f_{2n}}{2n+1} \qquad (2)$$

$$\langle cos^4 \beta \rangle = \sum_{n=0}^\infty \frac{f_{2n}}{2n+5} \Big/ \sum_{n=0}^\infty \frac{f_{2n}}{2n+1} \qquad (3)$$

$$\langle P2 \rangle = \frac{1}{2}(3\langle cos^2 \beta \rangle - 1) \qquad (4)$$

$$\langle P4 \rangle = \frac{1}{8}(35\langle cos^4 \beta \rangle - (30\langle cos^2 \beta \rangle + 3) \quad (5)$$

Results and discussion

Each material exhibits typical nematic and twist-bend scattering behaviour in non-resonant SAXS experiments, namely diffuse peaks at both wide and small angles. Representative 2D SAXS patterns are given in Fig 3. The small angle peak was found to be almost temperature invariant for all three compounds and to occur at a d-spacing of roughly 1/*n* the molecular length, with *n* corresponding to the number of mesogenic units per molecule (*i.e.* CB7CB n=2, **O4₇** n = 4, **O6₇** n = 6). The scattering at small angles in both mesophases is significantly more intense for the tetramer **O4₇** and the hexamer **O6₇** than for the dimer CB7CB; although the reason for this is unclear the simplest explanation would be that these materials experience a higher degree of cybotactic smectic fluctuations in both nematic and TB phases.
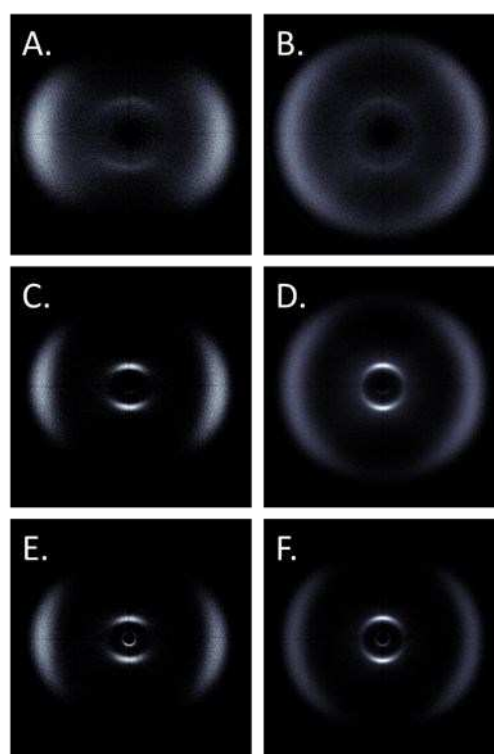
Fig 3: Magnetically aligned 2D SAXS patterns of: CB7CB in the nematic (A) and twist-bend phase (B); **O4₇** in the nematic (C) and twist-bend phase (D); **O6₇** in the nematic (E) and twist-bend phase (F). Each frame was recorded 5 °C below the N-Iso or TB-N transition.

All three materials were well aligned by the external magnetic field in both nematic and TB phases, permitting the measurement of order parameters as outlined in the experimental section. Plots of the order parameters $\langle P_2 \rangle$ and $\langle P_4 \rangle$ are given in Fig 4 as a function of reduced temperature (T / T$_{N\text{-}Iso}$) for the dimer CB7CB, the tetramer **O4₇** and the hexamer **O6₇**. For all materials at all temperatures studied we found $\langle P_6 \rangle$ to be below 0.01 and so values are omitted from these plots.

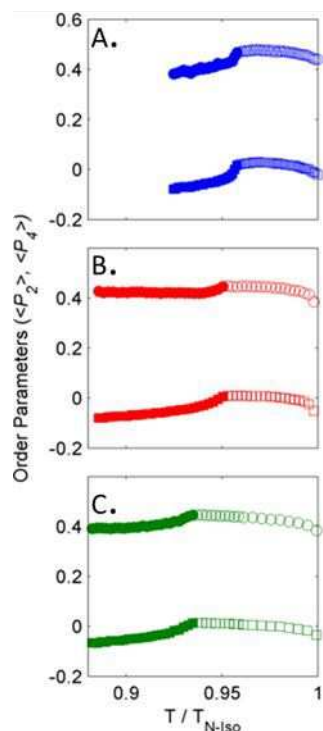Fig 4.   Plots of the order parameters $\langle P_2 \rangle$ (circles) and $\langle P_4 \rangle$ (squares) as a function of reduced temperature ($T / T_{N\text{-}Iso}$) for: (A) the dimer CB7CB; (B) the tetramer **O4₇**; (C) the hexamer **O6₇**. Empty data points correspond to values in the nematic phase, filled data points correspond to the twist-bend phase.

All three materials exhibit typical nematic order parameters throughout the nematic phase range; $\langle P_2 \rangle$ increases rapidly on cooling from the isotropic liquid and remains positive throughout, whereas $\langle P_4 \rangle$ takes a small negative value initially, changing sign and increasing in magnitude as the sample is cooled. The maximum values of both order parameters in the nematic phase occur immediately prior to the N-TB phase transition: all three materials have values of ~0.45 and ~0.15 for $\langle P_2 \rangle$ and $\langle P_4 \rangle$ at this point. As each sample is cooled into the twist-bend phase we find both $\langle P_2 \rangle$ and $\langle P_4 \rangle$ decrease, with $\langle P_4 \rangle$ becoming negative shortly after the N-TB phase transition. The decrease in both order parameters continues throughout the TB phase for CB7CB and the hexamer **O6₇**; the tetramer **O4₇** exhibits a decrease in $\langle P_4 \rangle$ of a similar magnitude, but $\langle P_2 \rangle$ remains constant at ~0.42. We note that order parameter values measured for CB7CB in this work compare favourably to prior data obtained by PRS [23] and SAXS. [24]

$$f(\beta) = \Sigma_0^\infty f_{2n} cos^{2n}\beta \qquad (6)$$

$$\int_0^\pi f(\beta) sin\beta d\beta = 1 \qquad (7)$$
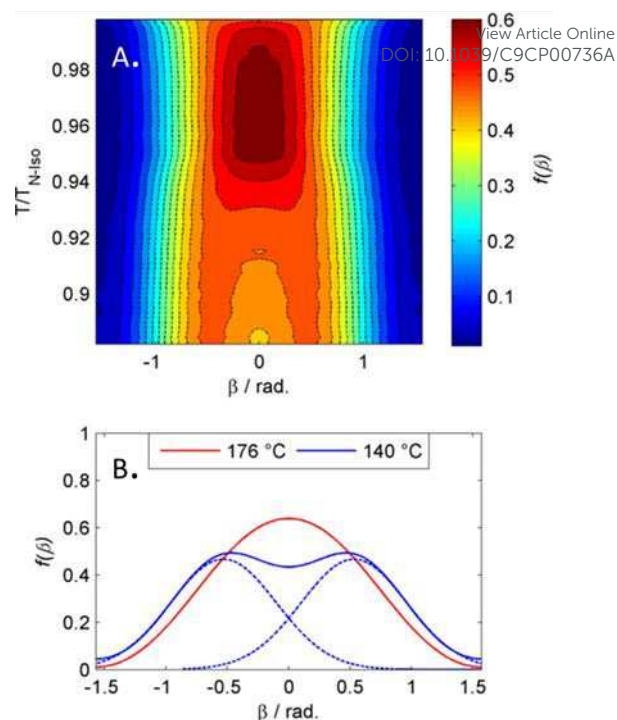

Fig 5:   (A) Contour plot of the ODF of the tetramer **O4₇** as a function of reduced temperature. (B) Plot of the ODF of **O4₇** at two temperatures; the volcano-like ODF was deconvoluted by fitting with two Gaussian peaks (dashed lines), the angular separation of which is twice the heliconical tilt angle (i.e. 2θ).

From coefficients used to determine the order parameters ($\langle P_2 \rangle$, $\langle P_4 \rangle$ and $\langle P_6 \rangle$) we can also calculate the truncated ODF ($f(\beta)$, Equation (6)) normalising the resulting values to Equation (7). In the nematic phase both $\langle P_2 \rangle$ and $\langle P_4 \rangle$ are positive and thus the ODF exhibits a typical sugarloaf-like shape (Fig 5a), being approximately Gaussian and centered at β=0. As both $\langle P_2 \rangle$ and $\langle P_4 \rangle$ decrease in the TB phase, with $\langle P_2 \rangle$ remaining positive and $\langle P_4 \rangle$ becoming negative, and this leads to a volcano-like ODF (Fig 5b) which is a consequence of the conical director distribution. These ODF plots represent a cross section of the helix, and thus the two maxima of the ODF depend upon the heliconical tilt angle. The two maxima correspond to the tilting of the mesogenic long axes away from the nematic director; therefore the average heliconical tilt angle is equal to half of this angular separation. [24] For all three materials in the TB phase the ODF was well fitted by two equal-width Gaussians, allowing the heliconical tilt angle to be determined. Plots of heliconical tilt angle as a function of reduced temperature are given in Fig 6.

We find CB7CB reaches a maximum heliconical tilt angle of 23 °, at which point the sample crystallises. Data for CB7CB is in good agreement with that obtained from SAXS by Sing et al., [24] and from both ^{129}Xe and ^{2}H NMR methods on CB7CB and CB7CB-d4, respectively. [25] We find that at any given reduced temperature our values of the heliconical tilt angle for CB7CB are about 5 ° smaller than those measured by birefringence measurements on large

monodomains of the TB phase. [26] We suggest this discrepancy may arise from the X-ray measurements being performed on a thick (capillary diameter of ~ 0.9 mm) polydomain sample.

The oligomeric materials **O4_7** and **O6_7** obtain maximum values of 28° and 29 °, respectively. It might be expected that a relationship exists between the heliconical tilt angle and the overall pitch length of the TB phase; that the heliconical tilt angle is similar for a dimer, a tetramer and a hexamer would therefore suggest that the pitch length for these materials is perhaps also similar, *i.e.* a few nanometers.
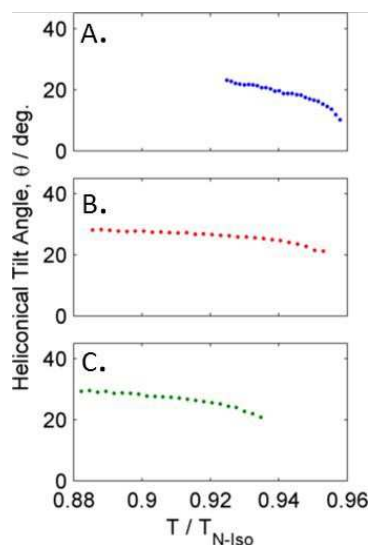

Fig 6.   Plots of the heliconical tilt angle (θ) as function of reduced temperature (T / T_{N-Iso}) for: (A) the dimer CB7CB; (B) the tetramer **O4_7**; (C) the hexamer **O6_7**.

One of the difficulties in proving the existence of the TB phase in a novel material is that unambiguous characterisation requires synchrotron X-ray techniques or freeze-fracture TEM to measure the heliconical pitch length. Measurement of the orientational order parameters and determination of the ODF and heliconical tilt angle outlined in this paper (and much earlier by Singh *et al* [24]) is straightforward and should help increase confidence in the identification of the TB phase in materials for which pitch length data is unavailable or impractical to obtain. Measurement of order parameters, ODF and tilt angles may provide powerful insight into the nature of the TB phase by studying (for example) the relationship between these features and gross bend angle, or the evolution of the conical tilt angle in materials with the phase sequence N-TB-SmA [27] or N-TB-SmC.

Conclusions

Using SAXS/WAXS we report on the temperature dependence of the orientational order parameters $\langle P_2 \rangle$ and $\langle P_4 \rangle$ for a liquid crystal dimer, tetramer and hexamer. For all three materials studied we find $\langle P_4 \rangle$ readily becomes negative in the TB phase as a

consequence of the conical local director in this phase. From SAXS/WAXS data we reconstruct the orientation distribution function for each material; whereas the nematic phase exhibits an approximately Gaussian distribution, it becomes 'volcano-like' in the TB phase as a consequence of the heliconical local structure. Fitting the ODF in the TB phase with two Gaussians allows us to measure the heliconical tilt angle as a function of temperature; remarkably the values obtained for CB7CB are not especially different to the tetramer **O4_7** or the hexamer **O6_7**.

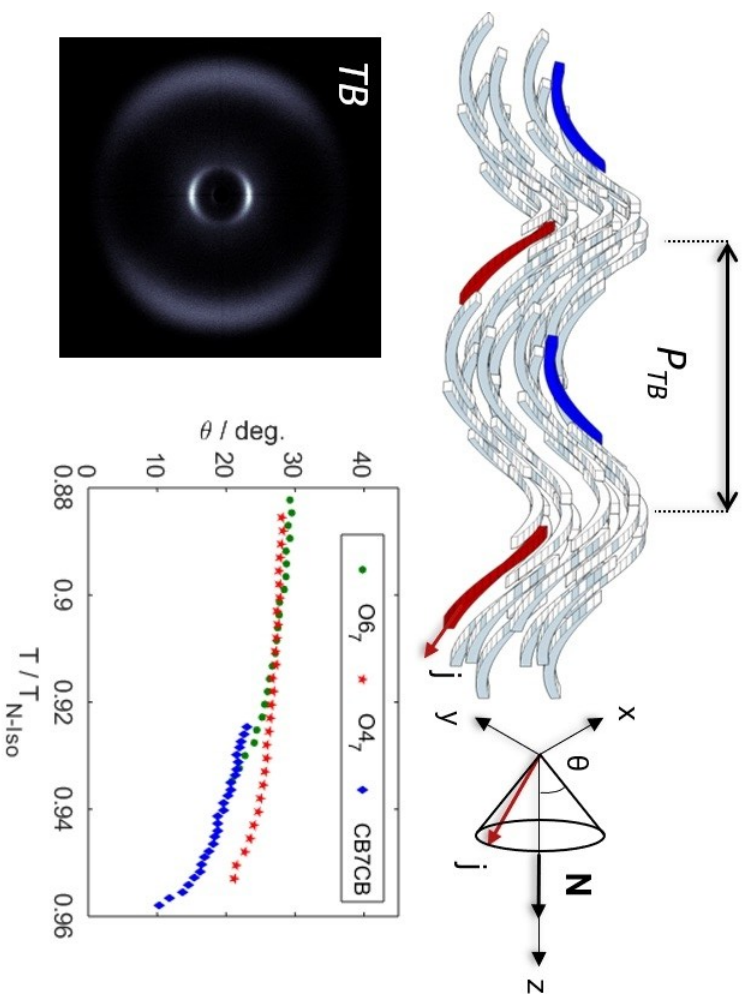## Conflicts of interest

There are no conflicts to declare

Notes and references

1.   I. Dozov, *Europhys Lett*, 2001, **56**, 247-253
2.   M. Cestari, S. Diez-Berart, D. A. Dunmur, A. Ferrarini, M. R. de la Fuente, D. J. Jackson, D. O. Lopez, G. R. Luckhurst, M. A. Perez-Jubindo, R. M. Richardson, J. Salud, B. A. Timimi and H. Zimmermann, *Phys Rev E Stat Nonlin Soft Matter Phys*, 2011, **84**, 031704
3.   M. Cestari, S. Diez-Berart, D. A. Dunmur, A. Ferrarini, M. R. de la Fuente, D. J. B. Jackson, D. O. Lopez, G. R. Luckhurst, M. A. Perez-Jubindo, R. M. Richardson, J. Salud, B. A. Timimi and H. Zimmermann, *Phys Rev E*, 2011, **84**
4.   D. Chen, J. H. Porada, J. B. Hooper, A. Klittnick, Y. Shen, M. R. Tuchband, E. Korblova, D. Bedrov, D. M. Walba, M. A. Glaser, J. E. Maclennan and N. A. Clark, *Proc Natl Acad Sci U S A*, 2013, **110**, 15931-15936
5.   C. Zhu, M. R. Tuchband, A. Young, M. Shuai, A. Scarbrough, D. M. Walba, J. E. Maclennan, C. Wang, A. Hexemer and N. A. Clark, *Phys Rev Lett*, 2016, **116**, 147803
6.   A. Jakli, O. D. Lavrentovich and J. V. Selinger, *Rev Mod Phys*, 2018, **90**
7.   J. W. Emsley, P. Lesot, G. R. Luckhurst, A. Meddour and D. Merlet, *Phys Rev E Stat Nonlin Soft Matter Phys*, 2013, **87**, 040501
8.   J. P. Abberley, R. Killah, R. Walker, J. M. D. Storey, C. T. Imrie, M. Salamonczyk, C. H. Zhu, E. Gorecka and D. Pociecha, *Nat Commun*, 2018, **9**
9.   R. J. Mandle, *Soft Matter*, 2016, **12**, 7883-7901
10. S. M. Jansze, A. Martinez-Felipe, J. M. D. Storey, A. T. M. Marcelis and C. T. Imrie, *Angew Chem Int Edit*, 2015, **54**, 643-646
11. Y. Wang, G. Singh, D. M. Agra-Kooijman, M. Gao, H. K. Bisoyi, C. M. Xue, M. R. Fisch, S. Kumar and Q. Li, *Crystengcomm*, 2015, **17**, 2778-2782
12. R. J. Mandle and J. W. Goodby, *Chemphyschem*, 2016, **17**, 967-970
13. A. Al-Janabi, R. J. Mandle and J. Goodby, *Rsc Adv*, 2017, **7**, 47235-47242
14. R. J. Mandle and J. W. Goodby, *Angewandte Chemie International Edition*, 2018, **57**, 7096-7100

ARTICLE

15. G. Ungar, V. Percec and M. Zuber, *Macromolecules*, 1992, **25**, 75-80

16. W. D. Stevenson, J. An, X. Zeng, M. Xue, H.-x. Zou, Y. Liu and G. Ungar, *Soft Matter*, 2018, **14**, 3003-3011

17. D. Chen, M. Nakata, R. Shao, M. R. Tuchband, M. Shuai, U. Baumeister, W. Weissflog, D. M. Walba, M. A. Glaser, J. E. Maclennan and N. A. Clark, *Phys Rev E Stat Nonlin Soft Matter Phys*, 2014, **89**, 022506

18. S. P. Sreenilayam, V. P. Panov, J. K. Vij and G. Shanker, *Liq Cryst*, 2016, DOI: 10.1080/02678292.2016.1253878, 1-10

19. C. T. Archbold, R. J. Mandle, J. L. Andrews, S. J. Cowling and J. W. Goodby, *Liq Cryst*, 2017, **44**, 2079-2088

20. F. P. Simpson, R. J. Mandle, J. N. Moore and J. W. Goodby, *J Mater Chem C*, 2017, DOI: 10.1039/C7TC00516D

21. M. T. Sims, L. C. Abbott, R. M. Richardson, J. W. Goodby and J. N. Moore, *Liq Cryst*, 2018, DOI: 10.1080/02678292.2018.1455227, 1-14

22. D. M. Agra-Kooijman, M. R. Fisch and S. Kumar, *Liq Cryst*, 2018, **45**, 680-686

23. Z. P. Zhang, V. P. Panov, M. Nagaraj, R. J. Mandle, J. W. Goodby, G. R. Luckhurst, J. C. Jones and H. F. Gleeson, *J Mater Chem C*, 2015, **3**, 10007-10016

24. G. Singh, J. X. Fu, D. M. Agra-Kooijman, J. K. Song, M. R. Vengatesan, M. Srinivasarao, M. R. Fisch and S. Kumar, *Phys Rev E*, 2016, **92**

25. J. P. Jokisaari, G. R. Luckhurst, B. A. Timimi, J. F. Zhu and H. Zimmermann, *Liq Cryst*, 2015, **42**, 708-721

26. C. Meyer, G. R. Luckhurst, and I. Dozov, *J. Mater. Chem. C,* 2015, **3**, 318-328

27. R. J. Mandle, E. J. Davis, S. A. Lobato, C. C. Vol, S. J. Cowling and J. W. Goodby, *Phys Chem Chem Phys*, 2014, **16**, 6907-6915

Physical Chemistry Chemical Physics Accepted Manuscript

141x107mm (150 x 150 DPI)